Preprints of the 21st IFAC World Congress (Virtual)
Berlin, Germany, July 12-17, 2020

Sectorial Fuzzy Controller Plus Feedforward applied to the Trajectory Tracking of Robot Manipulators ⋆

Andres O. Pizarro-Lerma * **Victor Santibanez** **
Ramon Garcia-Hernandez ** **Jorge Villalobos Chin** **

* *Instituto Tecnológico de Sonora, Cd. Obregón, Sonora 85000 México (e-mail: andres.pizarro@itson.edu.mx).*
** *Tecnológico Nacional de México/Instituto Tecnológico de La Laguna, Torreón, Coahuila 27000 México (e-mail: rgarciah@correo.itlalaguna.edu.mx, vsantiba@itlalaguna.edu.mx, santibanez@ieee.org, jorgevillaloboschin@hotmail.com)*

Abstract: In this paper, we propose a novel sectorial fuzzy controller plus feedforward for the trajectory tracking control of robot manipulators. An outline of the stability proof via Lyapunov criterion of the proposed controller is given. Experimental results are presented in comparison to its classical counterpart: The Proportional-Derivative (PD) plus feedforward controller, from which this new proposal is based. The results obtained using the proposed controller indicate a better performance in terms of joint position error and tolerance to parametric variations.

Keywords: Feedforward control, sectorial fuzzy controller, robot manipulator, trajectory tracking.

1. INTRODUCTION

Given the large number of industrial robots currently in use, applied to increasingly more exact and precise tasks (recode.net, 2017), it is necessary to find a controller capable of controlling the position of a robotic manipulator, such that it meets the task quality specifications. The control approaches still in use in many industrial applications are the Proportional + Integrator + Derivative (PID) control and its derivatives. A robot is highly nonlinear, with variations in its parameters almost at each point of execution. Within the various existing controller approaches to the motion control of robots, the Proportional + Derivative (PD) controller plus feedforward has great advantages on the elimination of disturbances, with an excellent tracking performance, comparable with that of the computed-torque controller (Kelly et al., 2005). Fuzzy controllers can be a robust and efficient alternative in cases where it is difficult to have an exact model of the plant to be controlled, or there are many disturbances and changes in some of its key parameters. Also, fuzzy control allows combining heuristic elements with analytical models. Once guidelines to design fuzzy controllers with sectorial properties, named Sectorial Fuzzy Controllers (SFC), which enable their stability analysis were given in Calcev (1998), many works on the motion control of robot manipulators emerged: In Santibanez et al. (2004), a computed torque control where its PD controller was exchanged by a SFC, showed excellent results in the tracking motion control of a 2-DOF Robot. A SFC with gravity compensation was applied to a robotic manipulator in order to regulate its joint positions in Santibanez et al. (2005), having excellent results. Our paper retakes the main idea of these previous works, as it presents the application of a PD controller plus feedforward for trajectory tracking control, where the PD part of the control law is replaced by a SFC, thus forming a novel SFC plus feedforward control, which has the properties and advantages of a SFC in relation to its tolerance to parameter deviation.

⋆ This work was supported in part by Programa para el Desarrollo Profesional Docente (PRODEP-México) under grant ITSON-126 and Tecnológico Nacional de México (TecNM) projects.

2. PRELIMINARIES

2.1 Dynamics of Robot Manipulators with rigid links

The dynamics of a serial n-link robot can be summarised by the Euler-Lagrange equations (Lewis et al., 2004), (Merabet and Gu, 2010) as:

$$\boldsymbol{M}(\boldsymbol{q})\ddot{\boldsymbol{q}} + \boldsymbol{C}(\boldsymbol{q},\dot{\boldsymbol{q}})\dot{\boldsymbol{q}} + \boldsymbol{g}(\boldsymbol{q}) + \boldsymbol{f}(\dot{\boldsymbol{q}}) = \boldsymbol{\tau} + \boldsymbol{\eta} \quad (1)$$

where $\boldsymbol{q}$ is the $n \times 1$ vector of angular positions at every joint in generalized coordinates and available for measurement, $\dot{\boldsymbol{q}}$ is the $n \times 1$ vector of joint angular velocities, $\ddot{\boldsymbol{q}}$ is the $n \times 1$ vector of joint angular accelerations, $\boldsymbol{\tau}$ is the $n \times 1$ vector of applied torques, $\boldsymbol{M(q)}$ is the $n \times n$ symmetric positive definite inertia matrix, $\boldsymbol{C}(\boldsymbol{q}, \dot{\boldsymbol{q}})\dot{\boldsymbol{q}}$ is the $n \times 1$ vector of centrifugal and Coriolis torques, $\boldsymbol{g}(\boldsymbol{q})$ is the vector of gravitational torques, $\boldsymbol{\eta}$ is the n-vector of uncertainties, which includes external disturbances, and all uncertainties in the parameters and dynamics not modelled in the robot; and $\boldsymbol{f}(\dot{\boldsymbol{q}})$ is the $n \times 1$ vector of friction torques. In the static models, friction is modelled by a vector $\boldsymbol{f}(\dot{\boldsymbol{q}}) \in \mathbb{R}^n$ that depends only on the joint velocity $\dot{\boldsymbol{q}}$ (Kelly et al., 2005). A

static friction model combines both viscous and Coulomb friction phenomena. This model states that the vector $\boldsymbol{f}(\dot{\boldsymbol{q}})$ is composed as

$$\boldsymbol{f}(\dot{\boldsymbol{q}}) = \boldsymbol{F_v}\dot{\boldsymbol{q}} + \boldsymbol{F_C}\ \mathrm{sgn}(\dot{\boldsymbol{q}}). \tag{2}$$

The diagonal elements of $\boldsymbol{F_v}$ are the viscous friction parameters, and the elements of $\boldsymbol{F_C}$ are the Coulomb friction parameters; both of them are $n \times n$ diagonal positive definite matrices. Where $\mathrm{sgn}(\dot{\boldsymbol{q}})$ denotes the vector sign function.

The dynamics of the n-link robot manipulator modelled by (1) has the following properties, which hold for manipulators having all rigid-link revolute joints (Slotine and Li, 1987), (Kelly et al., 2005),

Property A. The inertia matrix $\boldsymbol{M}(\boldsymbol{q})$ is symmetric and positive definite; that is,

$$\lambda_{\min}\{\boldsymbol{M}\}\|\boldsymbol{x}\|^2 \leq \boldsymbol{x}^T\boldsymbol{M}(\boldsymbol{q})\boldsymbol{x} \leq \lambda_{\max}\{\boldsymbol{M}\}\|\boldsymbol{x}\|^2 \tag{3}$$

where $\lambda_{\min}\{\boldsymbol{M}\} = \inf_q \lambda_{\min}\{\boldsymbol{M}(\boldsymbol{q})\}$, and $\lambda_{\max}\{\boldsymbol{M}\}$ denotes the $\sup_q \lambda_{\min}\{\boldsymbol{M}(\boldsymbol{q})\}$.

Property B. The vector $\boldsymbol{C}(\boldsymbol{q},\boldsymbol{x})\boldsymbol{y}$ satisfies the bound

$$\|\boldsymbol{C}(\boldsymbol{q},\boldsymbol{x})\boldsymbol{y}\| \leq k_{C1}\|\boldsymbol{x}\|\|\boldsymbol{y}\|,\ \forall\ \boldsymbol{q},\boldsymbol{x},\boldsymbol{y} \in \mathbb{R}^n;\quad k_{C1} > 0. \tag{4}$$

Property C. Assuming that the centrifugal and Coriolis torque matrix $\boldsymbol{C}(\boldsymbol{q},\dot{\boldsymbol{q}})\dot{\boldsymbol{q}}$ is computed by means of Christoffel symbols of the first kind. Then,

$$\boldsymbol{x}^T\left[\dot{\boldsymbol{M}} - 2\boldsymbol{C}(\boldsymbol{q},\dot{\boldsymbol{q}})\right]\boldsymbol{x} = 0\ \forall\ \boldsymbol{x},\boldsymbol{q},\dot{\boldsymbol{q}} \tag{5}$$

and,

$$\dot{\boldsymbol{M}} = \boldsymbol{C}(\boldsymbol{q},\dot{\boldsymbol{q}}) + \boldsymbol{C}(\boldsymbol{q},\dot{\boldsymbol{q}})^T. \tag{6}$$

Property D. The residual dynamics, $\boldsymbol{h}(\tilde{\boldsymbol{q}},\dot{\tilde{\boldsymbol{q}}})$, (Arimoto, 1995a),(Arimoto, 1995b), is defined as,

$$\begin{aligned}\boldsymbol{h}(\tilde{\boldsymbol{q}},\dot{\tilde{\boldsymbol{q}}}) =& \left[\boldsymbol{M}(\boldsymbol{q_d}) - \boldsymbol{M}(\boldsymbol{q})\right]\ddot{\boldsymbol{q}}_{\boldsymbol{d}} + \boldsymbol{g}(\boldsymbol{q_d}) - \boldsymbol{g}(\boldsymbol{q}) \\ &+ \left[\boldsymbol{C}(\boldsymbol{q_d},\dot{\boldsymbol{q}}_{\boldsymbol{d}}) - \boldsymbol{C}(\boldsymbol{q},\dot{\boldsymbol{q}})\right]\dot{\boldsymbol{q}}_{\boldsymbol{d}}\end{aligned} \tag{7}$$

where $\boldsymbol{q}_{\mathrm{d}}$ is the desired angular joint position, assumed to be three times differentiable with bounded derivatives for all time $t \geq 0$.

$$\tilde{\boldsymbol{q}} = \boldsymbol{q_d} - \boldsymbol{q} \tag{8}$$

is the angular joint position error.

The residual dynamics (7) has the property defined in (9) and satisfies the inequality in (10) (Kelly et al., 2005):

$$\boldsymbol{h}(\boldsymbol{0},\boldsymbol{0}) = \boldsymbol{0} \tag{9}$$

$$\|\boldsymbol{h}(\tilde{\boldsymbol{q}},\dot{\tilde{\boldsymbol{q}}})\| \leq k_{h1}\|\dot{\tilde{\boldsymbol{q}}}\| + k_{h2}\|\mathbf{tanh}\,(\tilde{\boldsymbol{q}})\| \tag{10}$$

where k_{h1} and k_{h2} are sufficiently large strictly positive constants that depend on the robot model parameters.

3. SECTORIAL FUZZY CONTROL PLUS FEEDFORWARD

The proposed Sectorial Fuzzy Control plus feedforward has a very similar configuration as a PD control plus feedforward, as described in (Kelly et al., 2005), except that the PD control is replaced by a Sectorial Fuzzy Control, as shown in Fig.1.

The control law for this controller is,

$$\begin{aligned}\boldsymbol{\tau} =& \boldsymbol{\Phi}(\tilde{\boldsymbol{q}},\dot{\tilde{\boldsymbol{q}}}) + \boldsymbol{M}(\boldsymbol{q_d})\ddot{\boldsymbol{q}}_{\boldsymbol{d}} \\ &+ \boldsymbol{C}(\boldsymbol{q_d},\dot{\boldsymbol{q}}_{\boldsymbol{d}})\dot{\boldsymbol{q}}_{\boldsymbol{d}} + \boldsymbol{g}(\boldsymbol{q_d}) + \boldsymbol{F_v}\dot{\boldsymbol{q}}_{\boldsymbol{d}}\end{aligned} \tag{11}$$

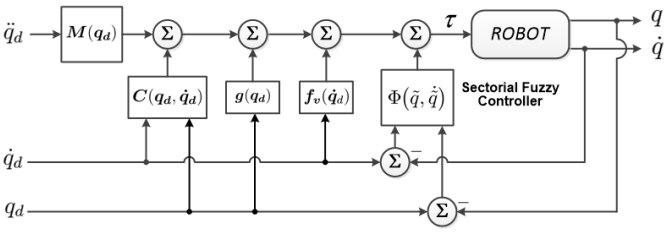

Fig. 1. Proposed Sectorial Fuzzy Control plus feedforward

where $\boldsymbol{\Phi}\left(\tilde{\boldsymbol{q}},\dot{\tilde{\boldsymbol{q}}}\right)$ is a $n \times 1$ vector whose elements $\phi_i\left(\tilde{q}_i,\dot{\tilde{q}}_i\right)$, with $i = 1,2,3,\ldots,n$, are the real input-output mappings of the Sectorial Fuzzy Control (SFC),

$$\boldsymbol{\Phi}\left(\tilde{\boldsymbol{q}},\dot{\tilde{\boldsymbol{q}}}\right) = \begin{bmatrix}\phi_1\left(\tilde{q}_1,\dot{\tilde{q}}_1\right) \\ \phi_2\left(\tilde{q}_2,\dot{\tilde{q}}_2\right) \\ \vdots \\ \phi_n\left(\tilde{q}_n,\dot{\tilde{q}}_n\right)\end{bmatrix}. \tag{12}$$

A SFC has one output related to two inputs, which from an input-output point of view forms a nonlinear static mapping with useful sectorial properties that enable the analysis of its stability. These sectorial properties have been well established and proven in Calcev (1998) and Santibanez et al. (2005), which are listed below:

- Property 1, $\phi(0,0) = 0$;
- Property 2, $\phi_i\left(\tilde{q}_i,\dot{\tilde{q}}_i\right) = -\phi_i\left(-\tilde{q}_i,-\dot{\tilde{q}}_i\right)$
- Property 3, There exist $\zeta_i,\rho_i > 0$, such that

$$0 < \tilde{q}_i\left[\phi_i\left(\tilde{q}_i,\dot{\tilde{q}}_i\right) - \phi_i\left(0,\dot{\tilde{q}}_i\right)\right] \leq \rho_i\tilde{q}_i^2$$
$$0 < \dot{\tilde{q}}_i\left[\phi_i\left(\tilde{q}_i,\dot{\tilde{q}}_i\right) - \phi_i\left(\tilde{q}_i,0\right)\right] \leq \zeta_i\dot{\tilde{q}}_i^2$$

- Property 4, $\phi_i\left(\tilde{q}_i,0\right) = 0 \Rightarrow \tilde{q}_i = 0$;
- Property 5, $\left|\phi_i\left(\tilde{q}_i,\dot{\tilde{q}}_i\right)\right| \leq \delta := max_{l1\ l2}\ \overline{y}^{l1\ l2}$;
- Property 6, $\overline{y}^{k\ 0} \leq \left|\phi_i\left(\tilde{q}_i,0\right)\right| \leq \overline{y}^{k+1\ 0}$;

for $i = 1,2,3,\ldots,n$, where $\overline{y}^{l1\ l2}, \overline{y}^{k\ 0}, \overline{y}^{k+1\ 0}$ represent the centres of the corresponding output membership functions (MF) that are defined during the design stage.

A SFC will have the properties listed before, if it is defined as follows: One output as a fuzzy mapping of two inputs. All MFs have to be symmetric with respect to zero, with an odd number of input and output fuzzy sets. The MF of adjacent input fuzzy sets must be defined so that they have complementary membership grades for every input value, as shown in figures 3 and 4 . The definition of fuzzy sets for the input MF must be convex in the sense given by (Calcev, 1998), and around zero no trapezoidal or similar MFs can be used. The consequents of the fuzzy rules table increase from left to right, and from top to bottom, with a null output for null inputs, as exemplified in table 1. The output is computed by the center average fuzzifier, applying the minimum or product inference method.

Also, from the properties stated before for a SFC, the following relationships can be expressed:

Recalling Property 3 of a SFC, evaluating $\tilde{q}_i = 0$, we have

$$\left|\phi_i\left(0,\dot{\tilde{q}}_i\right)\right| \leq \zeta_i \left|\dot{\tilde{q}}_i\right| \tag{13}$$

extrapolating (13) to the vector-matrix case, it leads to

$$\|\boldsymbol{\Phi}\left(\mathbf{0},\dot{\tilde{\boldsymbol{q}}}\right)\| \leq \lambda_{\mathrm{Max}}\{\boldsymbol{Z}\}\|\dot{\tilde{\boldsymbol{q}}}\| \tag{14}$$

where $\boldsymbol{Z} = \mathrm{diag}\{\zeta_i\}$ for $i = 1, 2, \ldots n$.
Letting $x_1 = \tilde{q}_i$ and $x_2 = \dot{\tilde{q}}_i$, such that $\phi(\tilde{q}_i, \dot{\tilde{q}}_i) = \phi(x_1, x_2)$, applying the guidelines for the definition of fuzzy rules given by Calcev (1998) and Santibanez et al. (2005), only four fuzzy rules will fire at a time, with related adjacent fuzzy sets k and $k+1$ for the input $x_1 = \tilde{q}_i$, and m, $m+1$ for $x_2 = \dot{\tilde{q}}_i$, then the output of the fuzzy block is computed, once simplified, as:

$$\begin{aligned}\phi(x_1,x_2) - \phi(0,x_2) = &\left[\bar{y}^{k,m} - \bar{y}^{0,m}\right] \\ &+ \underbrace{\mu_{A_1}^{k+1,}(x_1)\left[\bar{y}^{k+1,m} - \bar{y}^{k,m}\right]}_{\text{monotonic slope}}(x_1 - P_{1,k})\end{aligned} \tag{15}$$

where $\mu_{A_1}^{k+1}(x_m)$ represents the $k+1$ MF, which assigns a value to the membership grade of x_1 in the fuzzy set A_1; $P_{1,k}$ denotes the support values of the MFs, for the fuzzy set corresponding to $\tilde{q}$, as depicted in Fig. 3, that for triangular or trapezoidal MFs, which we are using in this paper, it is possible to prove that

$$|\phi_i(x_1,x_2) - \phi_i(0,x_2)| \geq \alpha_i \left|\tanh(x_1)\right| \tag{16}$$

where (Santibanez et al., 2004),

$$\alpha_i \leq \min_{j\neq 0}\left|\bar{y}^{k,j} - \bar{y}^{0,j}\right| \tag{17}$$

which leads to the following general expression

$$\|\boldsymbol{\Phi}(\tilde{\boldsymbol{q}},\dot{\tilde{\boldsymbol{q}}}) - \boldsymbol{\Phi}(\mathbf{0},\dot{\tilde{\boldsymbol{q}}})\| \geq \min_i\{\alpha_i\}\|\mathbf{tanh}\left(\tilde{\boldsymbol{q}}\right)\| \tag{18}$$

and from Property 3, $\mathrm{sign}\left(\Phi(\tilde{q}_i,\dot{\tilde{q}}_i) - \Phi(0,\dot{\tilde{q}}_i)\right) = \mathrm{sign}(\tilde{q}_i)$, therefore, in vectorial notation, we have

$$\begin{aligned}&\mathbf{tanh}\left(\tilde{\boldsymbol{q}}\right)^{\boldsymbol{T}}\left[\boldsymbol{\Phi}(\tilde{\boldsymbol{q}},\dot{\tilde{\boldsymbol{q}}}) - \boldsymbol{\Phi}(\mathbf{0},\dot{\tilde{\boldsymbol{q}}})\right] \geq \\ &\qquad \mathbf{tanh}\left(\tilde{\boldsymbol{q}}\right)^{\boldsymbol{T}}\boldsymbol{A}\,\mathbf{tanh}\left(\tilde{\boldsymbol{q}}\right) \geq \\ &\qquad \lambda_{\min}\{\boldsymbol{A}\}\|\mathbf{tanh}\left(\tilde{\boldsymbol{q}}\right)\|^2 > 0 \quad \forall\tilde{\boldsymbol{q}} \neq \mathbf{0} \in \mathbb{R}^n\end{aligned} \tag{19}$$

with $\boldsymbol{A} = \mathrm{diag}(\alpha_i)$

Also from (16), we have

$$|\phi_i(\tilde{q}_i,0)| \geq \alpha_i \left|\tanh(\tilde{q}_i)\right| \tag{20}$$

which in a general expression can be written as

$$\|\boldsymbol{\Phi}(\tilde{\boldsymbol{q}},\mathbf{0})\| \geq \lambda_{\min}\{\boldsymbol{A}\}\|\mathbf{tanh}\left(\tilde{\boldsymbol{q}}\right)\|. \tag{21}$$

4. STABILITY ANALYSIS OF THE SFC PLUS FEEDFORWARD CONTROLLER

The closed-loop equation of the system represented in the diagram shown in Fig. 1 is obtained by neglecting the Coulomb friction term, and combining (1) and (2) with the control law defined in (11), as

$$\boldsymbol{M}(\boldsymbol{q})\ddot{\boldsymbol{q}} + \boldsymbol{C}(\boldsymbol{q},\dot{\boldsymbol{q}})\dot{\boldsymbol{q}} + \boldsymbol{g}(\boldsymbol{q}) + \boldsymbol{F_v}\dot{\boldsymbol{q}} = \boldsymbol{\Phi}\left(\tilde{\boldsymbol{q}},\dot{\tilde{\boldsymbol{q}}}\right) + \boldsymbol{\tau_d} \tag{22}$$

with,

$$\boldsymbol{\tau_d} = \boldsymbol{M}(\boldsymbol{q_d})\ddot{\boldsymbol{q}}_{\boldsymbol{d}} + \boldsymbol{C}(\boldsymbol{q_d},\dot{\boldsymbol{q}}_{\boldsymbol{d}})\dot{\boldsymbol{q}}_{\boldsymbol{d}} + \boldsymbol{g}(\boldsymbol{q_d}) + \boldsymbol{F_v}\dot{\boldsymbol{q}}_{\boldsymbol{d}} \tag{23}$$

ans simplifying, in matrix form, the closed-loop system is given by

$$\frac{d}{dt}\begin{bmatrix}\tilde{\boldsymbol{q}}\\ \dot{\tilde{\boldsymbol{q}}}\end{bmatrix} = \begin{bmatrix}\dot{\tilde{\boldsymbol{q}}}\\ \boldsymbol{M}(\boldsymbol{q})^{-1}[-\boldsymbol{\Phi}\left(\tilde{\boldsymbol{q}},\dot{\tilde{\boldsymbol{q}}}\right) - \boldsymbol{C}(\boldsymbol{q},\dot{\boldsymbol{q}})\dot{\tilde{\boldsymbol{q}}} \\ -\boldsymbol{F_v}\dot{\tilde{\boldsymbol{q}}} - \boldsymbol{h}(\tilde{\boldsymbol{q}},\dot{\tilde{\boldsymbol{q}}})]\end{bmatrix}. \tag{24}$$

Theorem 1. The origin of the state space, $\left[\tilde{\boldsymbol{q}},\dot{\tilde{\boldsymbol{q}}}\right]$, is a globally uniformly asymptotically stable equilibrium of the closed loop system defined by (24), if the following conditions are met:

$$\lambda_{\min}\{\boldsymbol{A}\} > k_{h2} \tag{25}$$

$$\lambda_{\min}\{\boldsymbol{F_v}\} > \gamma\left(\sqrt{n}k_{C1} + \lambda_{\max}\{\boldsymbol{M}\}\right) + k_{h1} \tag{26}$$

$$0 < \gamma < \frac{\sqrt{\lambda_{\min}\{\boldsymbol{M}\}\lambda_{\min}\{\boldsymbol{AB}\}}}{\lambda_{\max}\{\boldsymbol{M}\}}. \tag{27}$$

Proof:
The equilibrium points of (24) are defined by

$$\{\tilde{\boldsymbol{q}} \in \mathbb{R}^n :\ 0 = \boldsymbol{\Phi}(\tilde{\boldsymbol{q}},\mathbf{0}) + \boldsymbol{h}(\tilde{\boldsymbol{q}},\mathbf{0}),\ \text{and}\ \dot{\tilde{\boldsymbol{q}}} = 0 \in \mathbb{R}^n\} \tag{28}$$

Where the origin is one equilibrium point. In order to carry out the stability analysis, we propose the following Lyapunov function candidate (LFC)

$$\begin{aligned}V(\tilde{\boldsymbol{q}},\dot{\tilde{\boldsymbol{q}}},t) = &\frac{1}{2}\dot{\tilde{\boldsymbol{q}}}^{\boldsymbol{T}}\boldsymbol{M}(\boldsymbol{q})\dot{\tilde{\boldsymbol{q}}} + \sum_{i=1}^{n}\int_0^{\tilde{q}_i}\phi(\xi_i,0)d\xi_i \\ &+ \gamma\,\mathbf{tanh}\left(\tilde{\boldsymbol{q}}\right)^{\boldsymbol{T}}\boldsymbol{M}(\boldsymbol{q})\dot{\tilde{\boldsymbol{q}}}.\end{aligned} \tag{29}$$

Now, applying (16), we have

$$\sum_{i=1}^{n}\int_0^{\tilde{q}_i}\phi(\xi_i,0)d\xi_i \geq \sum_{i=1}^{n}\alpha_i\int_0^{\tilde{q}_i}\tanh(\xi_i)d\xi_i \tag{30}$$

$$= \sum_{i=1}^{n}\alpha_i|\ln\left(\cosh(\tilde{q}_i)\right)| \geq \sum_{i=1}^{n}\alpha_i\beta_i|\tanh(\tilde{q}_i)|^2 \tag{31}$$

$$\geq \lambda_{\min}\{\boldsymbol{AB}\}\|\mathbf{tanh}\left(\tilde{\boldsymbol{q}}\right)\|^2. \tag{32}$$

In (31) we have used $\ln\{\cosh(\tilde{q}_i)\} \geq \beta_i\tanh(\tilde{q}_i)^2$, with $0 \leq \beta_i \leq \frac{1}{2}$, and $\boldsymbol{B} = \mathrm{diag}\{\beta_i\}$, for $i = 1, 2, \ldots n$. Using this result on (29), we have

$$\begin{aligned}V(\tilde{\boldsymbol{q}},\dot{\tilde{\boldsymbol{q}}},t) \geq &\frac{1}{2}\left(\lambda_{\min}\{\boldsymbol{M}\}\|\dot{\tilde{\boldsymbol{q}}}\|^2 + \lambda_{\min}\{\boldsymbol{AB}\}\|\mathbf{tanh}\left(\tilde{\boldsymbol{q}}\right)\|^2\right) \\ &+ \frac{1}{2}\sum_{i=1}^{n}\alpha_i|\ln\left(\cosh(\tilde{q}_i)\right)| - \gamma\lambda_{\max}\{\boldsymbol{M}\}\|\mathbf{tanh}\left(\tilde{\boldsymbol{q}}\right)\|\|\dot{\tilde{\boldsymbol{q}}}\|.\end{aligned}$$

In quadratic form,

$$V(\tilde{\boldsymbol{q}},\dot{\tilde{\boldsymbol{q}}},t) \geq \frac{1}{2}\left(g(\tilde{q}_i) + \begin{bmatrix}\|\mathbf{tanh}\left(\tilde{\boldsymbol{q}}\right)\| \\ \|\dot{\tilde{\boldsymbol{q}}}\|\end{bmatrix}^{\boldsymbol{T}}\boldsymbol{Q}\begin{bmatrix}\|\mathbf{tanh}\left(\tilde{\boldsymbol{q}}\right)\| \\ \|\dot{\tilde{\boldsymbol{q}}}\|\end{bmatrix}\right)$$

with $g(\tilde{q}_i) = \sum_{i=1}^{n}\alpha_i|\ln\left(\cosh(\tilde{q}_i)\right)|$, and

$$\boldsymbol{Q} = \begin{bmatrix}\lambda_{\min}\{\boldsymbol{AB}\} & -\gamma\lambda_{\max}\{\boldsymbol{M}\} \\ -\gamma\lambda_{\max}\{\boldsymbol{M}\} & \lambda_{\min}\{\boldsymbol{M}\}\end{bmatrix} \tag{33}$$

where $\boldsymbol{Q}$ is positive-definite if $\lambda_{\min}\{\boldsymbol{AB}\} > 0$, which is already fulfilled since $A, B > 0$ in their definitions, and if

$$\det\left(\boldsymbol{Q}\right) = \lambda_{\min}\{\boldsymbol{M}\}\lambda_{\min}\{\boldsymbol{AB}\} - \gamma^2\lambda_{\max}\{\boldsymbol{M}\}^2 > 0 \tag{34}$$

holds. Obtaining γ from (34),

$$0 < \gamma < \frac{\sqrt{\lambda_{\min}\{\boldsymbol{M}\}\lambda_{\min}\{\boldsymbol{AB}\}}}{\lambda_{\max}\{\boldsymbol{M}\}} \tag{35}$$

this value of γ ensures global positive definiteness of (29). Following similar steps is possible to prove that $V(\tilde{\boldsymbol{q}}, \dot{\tilde{\boldsymbol{q}}}, t)$ is a decrescent function. Therefore, (29) is a globally positive definite radially unbounded decrescent function which qualifies as a Lyapunov function candidate.

The time derivative of the LFC in (24) is

$$\begin{aligned}\dot{V}(\tilde{\boldsymbol{q}}, \dot{\tilde{\boldsymbol{q}}}, t) = &-\dot{\tilde{\boldsymbol{q}}}^{\boldsymbol{T}} \Big[\boldsymbol{\Phi}(\tilde{\boldsymbol{q}}, \dot{\tilde{\boldsymbol{q}}}) - \boldsymbol{\Phi}(\tilde{\boldsymbol{q}}, \boldsymbol{0})\Big] - \dot{\tilde{\boldsymbol{q}}}^{\boldsymbol{T}} \boldsymbol{h}(\tilde{\boldsymbol{q}}, \dot{\tilde{\boldsymbol{q}}}) \\ &- \gamma\, \mathbf{tanh}\,(\tilde{\boldsymbol{q}})^{\boldsymbol{T}} \boldsymbol{\Phi}(\tilde{\boldsymbol{q}}, \dot{\tilde{\boldsymbol{q}}}) - \dot{\tilde{\boldsymbol{q}}}^{\boldsymbol{T}} \boldsymbol{F_v} \dot{\tilde{\boldsymbol{q}}} \\ &- \gamma\, \mathbf{tanh}\,(\tilde{\boldsymbol{q}})^{\boldsymbol{T}} \boldsymbol{F_v} \dot{\tilde{\boldsymbol{q}}} - \gamma\, \mathbf{tanh}\,(\tilde{\boldsymbol{q}})^{\boldsymbol{T}} \boldsymbol{h}(\tilde{\boldsymbol{q}}, \dot{\tilde{\boldsymbol{q}}}) \\ &+ \gamma\, \mathbf{tanh}\,(\tilde{\boldsymbol{q}})^{\boldsymbol{T}} \boldsymbol{C}^{\boldsymbol{T}}(\tilde{\boldsymbol{q}}, \dot{\tilde{\boldsymbol{q}}}) \dot{\tilde{\boldsymbol{q}}} \\ &+ \gamma \dot{\tilde{\boldsymbol{q}}}^{\boldsymbol{T}} \mathbf{sech^2}(\tilde{\boldsymbol{q}}) \boldsymbol{M}(\boldsymbol{q}) \dot{\tilde{\boldsymbol{q}}}.\end{aligned} \tag{36}$$

Where we have used the Leibniz rule for differentiation of integrals. Applying the bounds defined in (4), (10) and the properties defined in (14) and (19) to simplify the expression, we have,

$$\begin{aligned}\dot{V}(\tilde{\boldsymbol{q}}, \dot{\tilde{\boldsymbol{q}}}, t) \leq &-\dot{\tilde{\boldsymbol{q}}}^{\boldsymbol{T}} \Big[\boldsymbol{\Phi}(\tilde{\boldsymbol{q}}, \dot{\tilde{\boldsymbol{q}}}) - \boldsymbol{\Phi}(\tilde{\boldsymbol{q}}, \boldsymbol{0})\Big] \\ &- \gamma \left(\lambda_{\min}\{\boldsymbol{A}\} - k_{h2}\right) \|\mathbf{tanh}\,(\tilde{\boldsymbol{q}})^2\| \\ &+ \gamma \left(\lambda_{\mathrm{Max}}\{\boldsymbol{Z}\} + \lambda_{\max}\{\boldsymbol{F_v}\} + \frac{k_{h2}}{\gamma} + k_{h1}\right. \\ &\left. + k_{C1} \|\dot{\boldsymbol{q}}_{\mathrm{M}}\|\right) \|\mathbf{tanh}\,(\tilde{\boldsymbol{q}})^T\| \|\dot{\tilde{\boldsymbol{q}}}\| \\ &- \gamma \left(\frac{\lambda_{\min}\{\boldsymbol{F_v}\} - k_{h1}}{\gamma} - \sqrt{n} k_{C1} - \lambda_{\max}\{\boldsymbol{M}\}\right) \|\dot{\tilde{\boldsymbol{q}}}\|^2.\end{aligned} \tag{37}$$

Defining the following constants,

$$a = \lambda_{\min}\{\boldsymbol{A}\} - k_{h2}, \quad b = k_{h2} \tag{38}$$

$$c = \lambda_{\mathrm{Max}}\{\boldsymbol{Z}\} + \lambda_{\max}\{\boldsymbol{F_v}\} + k_{h1} + k_{C1} \|\dot{\boldsymbol{q}}_{\mathrm{M}}\| \tag{39}$$

$$d = \lambda_{\min}\{\boldsymbol{F_v}\} - k_{h1}, \quad e = \sqrt{n} k_{C1} + \lambda_{\max}\{\boldsymbol{M}\} \tag{40}$$

and substituting them in (37), we have

$$\begin{aligned}\dot{V}(\tilde{\boldsymbol{q}}, \dot{\tilde{\boldsymbol{q}}}, t) \leq &-\dot{\tilde{\boldsymbol{q}}}^{\boldsymbol{T}} \Big[\boldsymbol{\Phi}(\tilde{\boldsymbol{q}}, \dot{\tilde{\boldsymbol{q}}}) - \boldsymbol{\Phi}(\tilde{\boldsymbol{q}}, \boldsymbol{0})\Big] \\ &- \gamma \begin{bmatrix} \|\mathbf{tanh}\,(\tilde{\boldsymbol{q}})\| \\ \|\dot{\tilde{\boldsymbol{q}}}\| \end{bmatrix}^T \underbrace{\begin{bmatrix} a & -\frac{\frac{b}{\gamma} + c}{2} \\ -\frac{\frac{b}{\gamma} + c}{2} & \frac{d}{\gamma} - e \end{bmatrix}}_{P_2} \begin{bmatrix} \|\mathbf{tanh}\,(\tilde{\boldsymbol{q}})\| \\ \|\dot{\tilde{\boldsymbol{q}}}\| \end{bmatrix}\end{aligned}$$

Since Property 3 of SFCs holds for the first term of $\dot{V}$, then $P_2 > 0 \implies \dot{V}(\tilde{\boldsymbol{q}}, \dot{\tilde{\boldsymbol{q}}}, t) < 0$. Therefore, we have the following relationships

$$\begin{aligned}&\lambda_{\min}\{\boldsymbol{A}\} > k_{h2} \implies a > 0 \\ &\lambda_{\min}\{\boldsymbol{F_v}\} > \gamma(\sqrt{n} k_{C1} + \lambda_{\max}\{\boldsymbol{M}\}) + k_{h1} \implies \\ &\quad \frac{d}{\gamma} - e > 0 \\ &\quad \det(P_2) > 0\end{aligned}$$

where,

$$\det(P_2) = a\left(\frac{d}{\gamma} - e\right) - \frac{\left(\frac{b}{\gamma} + c\right)^2}{4} > 0. \tag{41}$$

Obtaining $\lambda_{\min}\{\boldsymbol{A}\}$ from (38) and (41), we get:

$$\begin{aligned}&\lambda_{\min}\{\boldsymbol{A}\} > k_{h2} \\ &+ \frac{(b + \gamma c)^2}{4\gamma\left(\lambda_{\min}\{\boldsymbol{F_v}\} - \gamma\left[\sqrt{n} k_{C1} - \lambda_{\max}\{\boldsymbol{M}\}\right] - k_{h1}\right)}.\end{aligned} \tag{42}$$

If $\lambda_{\min}\{\boldsymbol{A}\}$ complies with (42), then $\dot{V} < 0$ which proves *Therorem 1.*

5. CONTROLLER DESIGN AND COMPARATIVE EXPERIMENTAL EVALUATION

5.1 2-DOF Robot Manipulator Description

A 2-DOF robot manipulator moving in the vertical plane, built in CICESE, México, and located at Instituto Tecnológico de La Laguna, México, shown in Fig. 2, was used to evaluate the performance of our controller. It consists of two rigid links, high-torque brushless direct-drive servos with no gear reduction, little backlash and very small joint friction. The maximum torque that can be applied to joint 1 is 150 [N–m], and 15 [N–m] for joint 2, according to the manufacturer (Reyes and Kelly, 2001).

The parameter values for this robot are, $l_1 = 0.450$ m, $l_2 = 0.450$ m, $l_{c1} = 0.091$ m, $l_{c2} = 0.091$ m, $m_1 = 23.902$ Kg, $m_2 = 3.880$ Kg, $I_1 = 1.266$ Kg m^2, $I_2 = 0.093$ Kg m^2, $fv_1 = 2.288$ N-m s, $fv_2 = 0.175$ N-m s, $g = 9.81$ m/s^2.

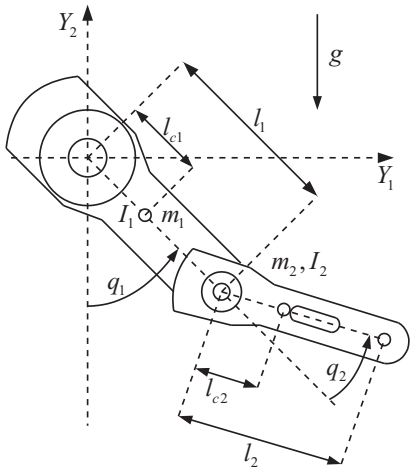

Fig. 2. Diagram of the 2-DOF robot manipulator used in the experiments

The dynamical model of the robot shown in Fig. 2 can be expressed as in (1), with

$$\begin{aligned}M_{11}(q) &= m_1 l_{c1}^2 + m_2[l_1^2 + l_{c2}^2 + 2 l_1 l_{c2} \cos(q_2)] + I_1 + I_2, \\ M_{12}(q) &= m_2[l_{c2}^2 + l_1 l_{c2} \cos(q_2)] + I_2, \\ M_{21}(q) &= m_2[l_{c2}^2 + l_1 l_{c2} \cos(q_2)] + I_2, \\ M_{22}(q) &= m_2 l_{c2}^2 + I_2, \\ C_{11}(q, \dot{q}) &= -m_2 l_1 l_{c2} \sin(q_2) \dot{q}_2, \\ C_{12}(q, \dot{q}) &= -m_2 l_1 l_{c2} \sin(q_2)[\dot{q}_1 + \dot{q}_2], \\ C_{21}(q, \dot{q}) &= -m_2 l_1 l_{c2} \sin(q_2) \dot{q}_1, \\ C_{22}(q, \dot{q}) &= 0, \\ g_1(q) &= [m_1 l_{c1} + m_2 l_1] g \sin(q_1) + m_2 l_{c2}\, g \sin(q_1 + q_2), \\ g_2(q) &= m_2 l_{c2} g \sin(q_1 + q_2).\end{aligned}$$

In our controller definition and implementation, only the viscous friction, $\boldsymbol{F_v}$, is considered. The Coulomb friction, $\boldsymbol{F_C}$, was only taken into account within the robot model for simulation purposes, and beyond that, it will be further taken as a disturbance, as was discussed in previous sections.

5.2 SFC plus Feedforward Controller Design

Fuzzy MFs for each input of each joint were defined as it is shown in figures 3 and 4. Also, the definition of the torque output fuzzy MF for each joint is shown in Fig. 5. We used singletons to define the output fuzzy MF in order to expedite its computation when implemented in real-time. In our definition of fuzzy sets, the acronyms used in each MF for both the two inputs and the output, are: NB = Negative Big, NS = Negative Small, Z = Zero, PS = Positive Small, and PB = Positive Big.

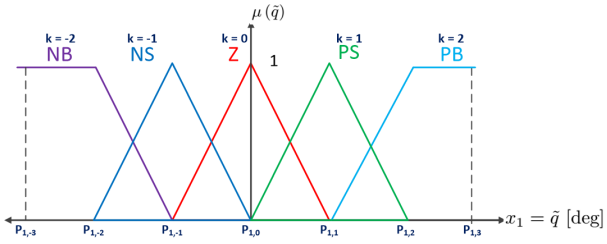

Fig. 3. Definition of fuzzy sets for $x_1 = \tilde{q}_i$

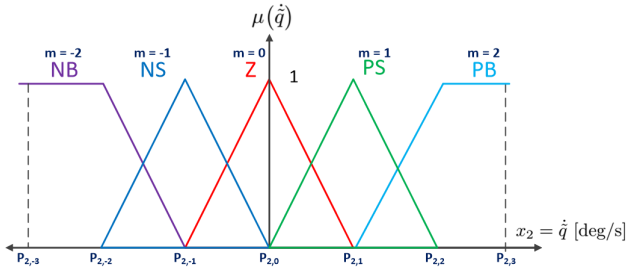

Fig. 4. Definition of fuzzy sets for $x_2 = \dot{\tilde{q}}_i$

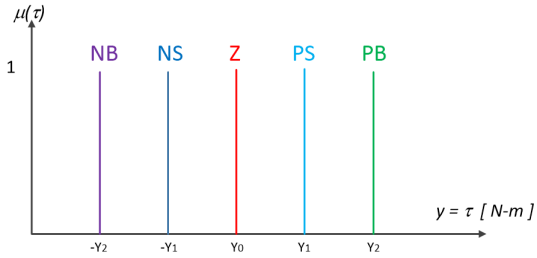

Fig. 5. Definition of fuzzy sets for the output τ

Table 1 shows the fuzzy rules. They were defined following the guidelines in Calcev (1998) so that our fuzzy controller has the sectorial properties described in section 3.

The values that define the fuzzy sets for both joints were found applying Genetic Algorithms (GA), as in Pizarro et al. (2018). The 2-DOF robot manipulator from Fig. 2 was used as our plant, where both viscous and Coulomb friction were included within its model, used in the ensuing simulations required for the optimisation process. The

Table 1. Fuzzy rules look-up table

$\dot{\tilde{q}}/\tilde{q}$	NB	NS	Z	PS	PB
NB	NB	NB	NS	Z	Z
NS	NB	NB	NS	Z	Z
Z	NS	NS	Z	PS	PS
PS	Z	Z	PS	PB	PB
PB	Z	Z	PS	PB	PB

support values for the fuzzy sets obtained via GA are: $P_{1,0} = 0$, $P_{1,1} = 6.518$, $P_{1,2} = 53.77$, $P_{1,3} = 125.5$, $P_{2,0} = 0$, $P_{2,1} = 122.2$, $P_{2,2} = 138.5$ $P_{2,3} = 871.8$, $Y_0 = 0$, $Y_1 = 82.29$, $Y_2 = 204.5$, for joint 1; and $P_{1,0} = 0$, $P_{1,1} = 5.982$, $P_{1,2} = 36.67$ $P_{1,3} = 163.5$, $P_{2,0} = 0$, $P_{2,1} = 153.8$, $P_{2,2} = 318.7$ $P_{2,3} = 1016$, $Y_0 = 0$, $Y_1 = 15$, $Y_2 = 180$, for joint 2.

5.3 Comparative Experimental Evaluation

The desired joint position vector, $\boldsymbol{q_d}(t)$, is given by the next equations, according to the values and functions recommended in Kelly et al. (2005) for this type of tests:

$$q_{1\mathrm{d}}(t) = d_1 + k_1(1 - e^{-2t^3}) + k_3(1 - e^{-2t^3})\mathrm{sen}(\omega_1 t) \text{ [rad]}$$

$$q_{2\mathrm{d}}(t) = d_2 + k_2(1 - e^{-1.8t^3}) + k_4(1 - e^{-1.8t^3})\mathrm{sen}(\omega_2 t) \text{ [rad]}$$

where $d_1 = \pi/2$ [rad], $k_1 = \pi/4$ [rad], $k_3 = \pi/18$ [rad], $\omega_1 = 15$ [rad/s], $d_2 = \pi/2$ [rad], $k_2 = \pi/3$ [rad], $k_4 = 25\pi/36$ [rad] and $\omega_2 = 3.5$ [rad/s].

From the desired joint positions vector, $\boldsymbol{q_d}(t)$, desired joint velocities and accelerations vectors, $\dot{\boldsymbol{q}}_{\boldsymbol{d}}(t)$ and $\ddot{\boldsymbol{q}}_{\boldsymbol{d}}(t)$, were analytically computed by calculating their derivatives.

We also designed a PD plus feedforward controller to comparatively test its performance versus the SFC plus feedforward. The elements of the gain matrices $\boldsymbol{K_p}, \boldsymbol{K_v} \in \mathbb{R}^{2\times 2}$ were obtained using the same optimising method of GA, as in the case of the SFC, but adapted to a PD case. This optimisation yielded the values:

$$\boldsymbol{K_p} = \mathrm{diag}\{70.7137, 41.7283\} \quad \boldsymbol{K_v} = \mathrm{diag}\{11.1162, 4.377\}$$

Both controllers previously designed and simulated were executed on WinMechLab, a real–time platform running on Windows 7 (Campa et al., 2004), with a 2.5 ms sampling period, and using a MultiQ-PCI data acquisition board from Quanser Consulting Inc. The angular position error responses were obtained for each joint, as well as the applied torques as shown in figures 6–9.

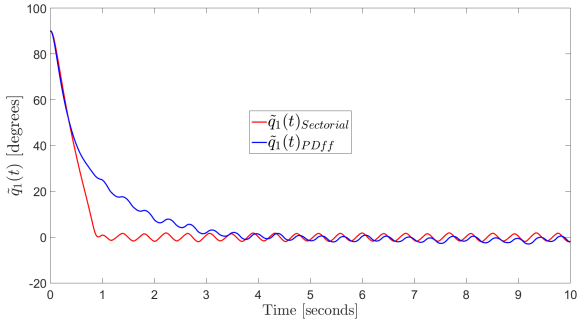

Fig. 6. Position error for joint 1

In table 2, a comparison of the RMS position error in each joint is shown for every controller, where "ss" stands for

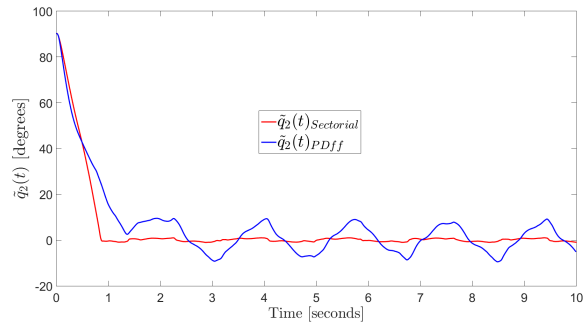

Fig. 7. Position error for joint 2

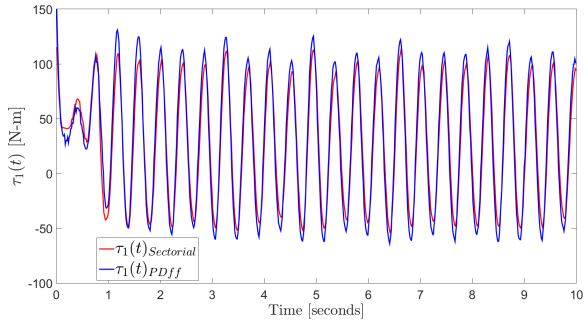

Fig. 8. Applied torque to joint 1

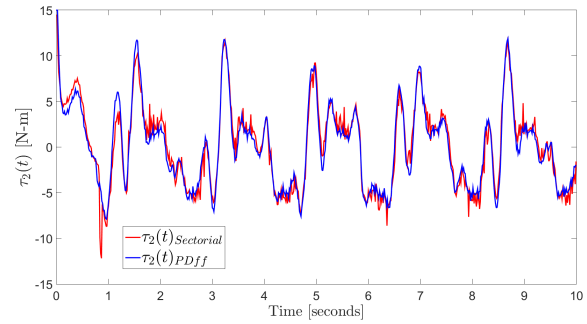

Fig. 9. Applied torque to joint 2

steady-state values, computed from 5 seconds to the end of the experiment.

Table 2. RMS Position Error Comparative

Controller	$\tilde{q}_1$	$\tilde{q}_{1,ss}$	$\tilde{q}_2$	$\tilde{q}_{2,ss}$
PD+ff	17.1754	1.4021	17.1683	5.3036
Sectorial	15.218	1.1867	15.9701	0.6256

For all joints, position errors have smaller values for the SFC plus feedforward, labeled as 'Sectorial' in both the comparative table and figures, than for the PD plus feedforward controller, labeled PD+ff. Applied torques in both joints have similar values (as in joint 2), or are generally smaller (joint 1 case) for our proposed SFC plus feedforward.

6. CONCLUSION

A novel SFC plus feedforward, applied to the trajectory tracking control of a robot manipulator, including an outline of its stability prof, has been presented for the first time. We have successfully evaluated it experimentally, without the need for any parameter tuning, that was not the case with its PD counterpart, which indeed needed to be tuned several times before achieving a similar response to the one obtained in simulations.

ACKNOWLEDGEMENTS

The authors thank PRODEP and TecNM projects for the support given to carry out this work.

REFERENCES

Arimoto, S. (1995a). Fundamental problems of robot control: Part I, innovations in the realm of robot servo-loops. *Robotica*, 13(1), 19–27.

Arimoto, S. (1995b). Fundamental problems of robot control: Part II a nonlinear circuit theory towards an understanding of dexterous motions. *Robotica*, 13(2), 111–112.

Calcev, G. (1998). Some remarks on the stability of mamdani fuzzy control systems. *IEEE Trans. Fuzzy Syst.*, 6, 436–442.

Campa, R., Kelly, R., and Santibanez, V. (2004). Windows-based real-time control of direct-drive mechanisms: platform description and experiments. *Mechatronics*, 14, 1021–1036.

Kelly, R., Santibanez, V., and Loria, A. (2005). *Control of Robot Manipulators in Joint Space*. Springer-Verlag London Limited, Germany.

Lewis, F.L., Dawson, D.M., and Abdallah, C.T. (2004). *Robot Manipulator Control, Theory and Practice, 2nd Edition, Revised and Expanded*. Marcel Dekker, Inc., NewYork and Basel.

Merabet, A. and Gu, J. (2010). *Advanced Nonlinear Control of Robot Manipulators, Robot Manipulators New Achievements*. InTech, www.intechopen.com.

Pizarro, A., Garcia-Hernandez, R., and Santibanez, V. (2018). Fine-tuning of a fuzzy computed-torque control for a 2-dof robot via genetic algorithms. *Proceedings of the Second IFAC Conference on Modelling, Identification and Control of Nonlinear Systems*, 1, 326–331.

recode.net (2017). The number of robots sold in the U.S. will jump nearly 300 percent in nine years. *https://www.recode.net*, 1(1), 1–9.

Reyes, F. and Kelly, R. (2001). Experimental evaluation of model-based controllers on a drive robot arm. *Mechatronics*, 11(1), 267—-282.

Santibanez, V., Kelly, R., and Llama, M. (2004). Global asymptotic stability of a tracking sectorial fuzzy controller for robot manipulators. *IEEE Transactions on Systems, Man, and Cybernetics Part B: Cybernetics*, 34, 710 – 718.

Santibanez, V., Kelly, R., and Llama, M.A. (2005). A novel global asymptotic stable set-point fuzzy controller with bounded torques for robot manipulators. *IEEE Transactions on Fuzzy Systems*, 13, 362–372.

Slotine, J.E. and Li, W. (1987). On the adaptive control of robot manipulators. *The International Journal of Robotics Research*, 6, 49–59.